 CMC, vol.5, no.2, pp.117-127, 2007

Wave Propagation around Thin Structures using the MFS

L. Godinho[1], A. Tadeu[1] and P. Amado Mendes[1]

Abstract: This paper presents a strategy for using the Method of Fundamental Solutions (MFS) to model the propagation of elastic waves around thin structures, like empty cracks or thin rigid screens, located in a homogeneous elastic medium. The authors make use of a simple approach for modeling these propagation conditions using the MFS together with decomposition of the domain into distinct regions. This approach makes it possible to avoid the undetermined system of equations that arises from imposing boundary conditions at both sides of a thin structure. The numerical implementation of the MFS is performed in the frequency domain, making use of the Fundamental Solutions defined by Tadeu and Kausel (2000) for the propagation of elastic waves generated by a 2.5D load located in an unbounded domain. Using this formulation, it is then possible to model 3D structures which have a constant cross-section in the z direction. This calculation is performed by decomposing the 3D response into a sequence of 2D responses computed for different wave-numbers along z.

The first part of the paper describes the formulation of the method in detail, also presenting the Fundamental Solutions used. Then, the method is verified by comparing its results against those given by a frequency domain formulation of the Traction Boundary Element Method (TBEM).

A final section of the paper presents a sample application which illustrates the applicability of the method to study the wave propagation around a thin rigid screen, embedded in a fluid medium. For this case, time domain responses are computed and presented in the form of snapshots.

Keyword: MFS, thin structures, domain decomposition.

[1] Dept. Civil Eng., Univ. Coimbra

1 Introduction

The use of numerical methods has proved to be extremely useful in many physical problems, since they allow the simulation of complex geometries and material behaviors. Over the past years, the Finite Element Method (FEM) and the Finite Difference Method (FDM) have been extensively used in almost every domain of science and engineering. However, in some specific domains other numerical methods have proved to be more effective. Some of these methods, like the Boundary Element Method, have been the object of extensive research. In fact, for the analysis of acoustic or elastic wave propagation, the BEM has emerged in the past twenty years as one of the dominant techniques, particularly in configurations that involve unbounded or semi-infinite media (see, for example, Tadeu and Godinho, 2003).

One of the most important advantages of the BEM over its counterparts, especially the FEM and FDM, is that it only requires the discretization of the boundary interfaces. One drawback of the method is its mathematical complexity, since it requires the prior knowledge of the fundamental solutions, i.e Green's functions, for the physical problem. These fundamental solutions can only be determined for certain specific types of differential equations, and it becomes very difficult to derive them when the physical domain to be analyzed is not homogeneous. A second drawback of the BEM is that its formulation requires the evaluation of singular and hyper-singular integrals along the boundary. Handling these integrations generally requires elaborate numerical schemes together with mathematical manipulation of the expressions, or, in some cases, their analytical evaluation. For a few cases, such as frequency domain wave propagation problems that

use straight boundary elements, analytical solutions for these integrals have been proposed by Tadeu et el (1999a, 1999b), when the integrations involve the loaded element.

Latterly, a significant effort has been put into the development of a different class of numerical methods, usually known as meshless or mesh-free methods. In essence, these new methods require neither domain nor boundary discretization. A few examples of these techniques are: the method of fundamental solutions (MFS) [Fairweather et al. (1998), Golberg et al. (1999)], the radial basis functions (RBF) collocation method [Kansa (1990)], and the Meshless Local Petrov-Galerkin method [Atluri (2004)].

The authors of the present paper focus on the use of the MFS to study wave propagation in solids and fluids. The formulation of this method is mathematically very simple, although it requires prior knowledge of the fundamental solutions for the physical problem to be studied. It can be viewed as an indirect BEM since it is solved after satisfying the boundary conditions. However, no numerical integration is needed along the boundaries, which avoids the difficulty posed by singular and hyper-singular integrations. Previous work by the authors of this paper [Godinho et al (2006)] has studied the performance of the MFS for simulating the propagation of acoustic waves in a fluid domain with an inclusion, concluding that the method can be very efficient, even surpassing the performance of the BEM for this type of problem.

A specific class of problems within the field of wave propagation involves the propagation of both elastic and acoustic waves around cracks or thin rigid bodies. Studying this type of geometry usually requires even more complex boundary element formulations, such as the Traction Boundary Element Method (TBEM), to avoid the singularities that arise in the classic boundary element formulation for these situations. In recent work by Tadeu et al (2006) and Amado Mendes et al (2006), this methodology has been extensively developed and implemented to model wave propagation around thin structures with rigid or free boundaries, located inside fluid or elastic domains. But a very simple alternative can be used, which consists of decomposing the propagation domain into different sub-domains, in such a way that the two opposite boundaries of the thin structures face different sub-domains. This general technique has been known for some years [see, for example, Brebbia and Dominguez (1989)], and it can be applied to a wide variety of physical problems. In theory, it can also be used together with the MFS, thus allowing the simulation of such configurations. However, a recent study by Leitão and Alves (2006) concluded that, in the specific case of 2D static torsion in solids with a crack, the described approach does not yield accurate results, and the simulation of such problems would require the use of so-called enrichment functions.

In the present paper, the authors study the applicability of a domain decomposition technique together with the MFS to simulate wave propagation in solids and fluids with embedded thin structures. In all cases, the medium is assumed to be two-dimensional, while the dynamic source is three-dimensional (e.g. a point load). Such a situation is frequently referred to as a two-and-a-half-dimensional problem (or 2-1/2-D for short), and solutions can be obtained for this by means of a 2D spatial Fourier transform in the direction in which the geometry does not vary [Tadeu and Godinho (1999)].

For the purpose of this study, the MFS and TBEM solutions for the analysis of a semicircular crack inside an unbounded solid domain and for a semicircular rigid thin screen located within an unbounded fluid will be compared.

First, the three-dimensional problem is formulated. Then, a brief description of the mathematical formulation of the MFS is given, together with the fundamental solutions for the problems to be solved. There follows an explanation of the domain decomposition approach used here. Then, a selection of numerical results is presented to assess the accuracy of the proposed approach. A sample numerical application is then presented, which identifies the most important characteristics of wave propagation around a thin structure.

2 2.5D Frequency domain problem formulation

Consider a cylindrical elastic inclusion of infinite extent, subjected to a harmonic point pressure source at position $(x_0,0,0)$, oscillating with frequency ω. The incident field can be expressed by means of the now classical dilatational potential ϕ

$$\phi_{inc} = \frac{A e^{i\frac{\omega}{\alpha}\left(\alpha t - \sqrt{(x-x_0)^2+y^2+z^2}\right)}}{\sqrt{(x-x_0)^2+y^2+z^2}} \tag{1}$$

where the subscript *inc* denotes the incident field, A is the wave amplitude, α is the compressional wave velocity of the medium, and $i=\sqrt{-1}$.

Defining the effective wavenumbers $k_\alpha = \sqrt{\frac{\omega^2}{\alpha^2}-k_z^2}$, $Imk_\alpha < 0$ by means of the axial wavenumber k_z, and Fourier-transforming equation (1) in the z direction, we obtain

$$\hat{\phi}_{inc}(\omega,x,y,k_z) = \frac{-iA}{2} H_0^{(2)}\left(k_\alpha \sqrt{(x-x_0)^2+y^2}\right) \tag{2}$$

where $H_n^{(2)}(\cdots)$ are second Hankel functions of order n.

If an infinite set of periodically placed sources along the z direction at equal intervals, L, is considered, the incident field may be written as

$$\phi_{inc}(\omega,x,y,z) = \frac{2\pi}{L}\sum_{m=-\infty}^{\infty} \hat{\phi}_{inc}(\omega,x,y,k_z) e^{-ik_{zm}z} \tag{3}$$

with $k_{zm} = \frac{2\pi}{L}m$, that converges and can be approximated by a finite sum of terms.

3 Formulation of the MFS

3.1 General formulation

For the MFS, the solution is approximated throughout the domain in terms of a linear combination of fundamental solutions for the governing equation. So, in an acoustic domain, the pressure field can be written as

$$p^{(1)}(x,y) = \sum_{n=1}^{NS} Q_n G^{(1)}(\omega, x_n^{(2)}, y_n^{(2)}, x, y, k_z) \tag{4}$$

$$p^{(2)}(x,y) = \sum_{n=1}^{NS} P_n G^{(2)}(\omega, x_n^{(1)}, y_n^{(1)}, x, y, k_z) \tag{5}$$

where $(x_n^{(i)}, y_n^{(i)})$ are the coordinates of NS distinct source points placed along a fictitious boundary of the medium i (see Figure 1); Q_n and P_n are the amplitudes to determined for the source points. The functions $G^{(i)}(\cdots)$ are the fundamental solutions for acoustic wave propagation in the medium i. For 2.5D problems, these solutions can be given as

$$G(\omega,x_n,y_n,x,y,k_z) = -\frac{i}{4} H_0^{(2)}\left(\sqrt{\left(\frac{\omega^2}{c^2}-k_z^2\right)}\sqrt{(x-x_n)^2+(y-y_n)^2}\right) \tag{6}$$

with $\mathrm{Im}\left(\sqrt{\left(\frac{\omega^2}{c^2}-k_z^2\right)}\right) \le 0$.

In order to avoid singularities, the fictitious sources are placed outside the domain of the problem. Two different approaches have been described in the literature for choosing their positions: fixed, and adaptive [Fairweather et al (1998); Golberg et al (1999)]. In the present paper, the source points are chosen a priori using a fixed scheme. Since only circular geometries will be studied, the source points are equally spaced around circles with the same center as the inclusion.

Similarly, for an elastic inclusion inside an elastic infinite domain the displacement field can be written as

$$u_i^{(1)}(x,y) = \sum_{n=1}^{NS}\sum_{j=1}^{3} P_{nj} G_{ij}^{(1)}(\omega, x_n^{(2)}, y_n^{(2)}, x, y, k_z) \tag{7}$$

$$u_i^{(2)}(x,y) = \sum_{n=1}^{NS}\sum_{j=1}^{3} Q_{nj} G_{ij}^{(2)}(\omega, x_n^{(1)}, y_n^{(1)}, x, y, k_z) \tag{8}$$

In these equations, $G_{ij}(\omega,x_n,y_n,x,y,k_z)$ (i,j =1, 2, 3) are the displacements in direction j at (x,y), caused by a unit point force applied at (x_n,y_n).

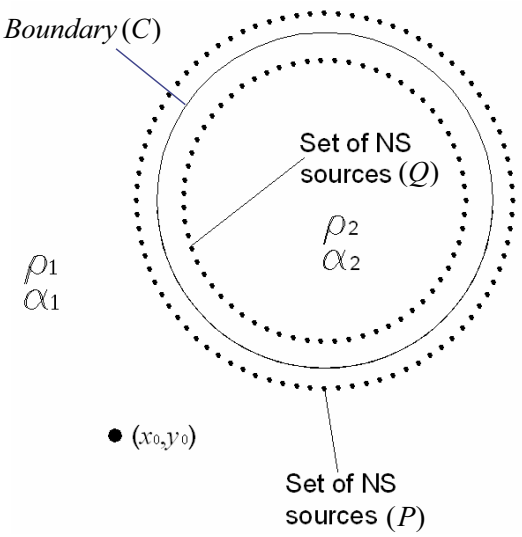

Figure 1: Physical domain and fictitious boundary.

The fictitious sources are placed outside the propagation domain of the problem to avoid singularities.

The fundamental solutions for this problem are known, and their mathematical derivation can be found in Tadeu and Kausel (2000). For completeness, the mathematical expressions of these fundamental solutions are presented in equations (9) to (14).

$$G_{xx} = A\left[k_s^2 H_{0\beta} - \frac{1}{r}B_1 + \gamma_x^2 B_2\right] \tag{9}$$

$$G_{yy} = A\left[k_s^2 H_{0\beta} - \frac{1}{r}B_1 + \gamma_y^2 B_2\right] \tag{10}$$

$$G_{zz} = A\left[k_s^2 H_{0\beta} - k_z^2 B_0\right] \tag{11}$$

$$G_{xy} = G_{yx} = \gamma_x \gamma_y A B_2 \tag{12}$$

$$G_{xz} = G_{zx} = \mathrm{i}k_z \gamma_x A B_1 \tag{13}$$

$$G_{yz} = G_{zy} = \mathrm{i}k_z \gamma_y A B_1 \tag{14}$$

where λ and μ are Lamé constants, ρ is the mass density, $\alpha = \sqrt{(\lambda+2\mu)/\rho}$ is the P wave velocity, $\beta = \sqrt{\mu/\rho}$ is the S wave velocity, $k_p = \omega/\alpha$ and $k_s = \omega/\beta$ are the compressional and shear wave numbers, $k_\alpha = \sqrt{k_p^2 - k_z^2}$, $k_\beta = \sqrt{k_s^2 - k_z^2}$, $A = \frac{1}{4\mathrm{i}\rho\omega^2}$, $\gamma_i = \frac{\partial r}{\partial x_i} = \frac{x_i}{r}$ with $i = 1, 2$, $H_{n\alpha} = \mathrm{H}_n^{(2)}(k_\alpha r)$, $H_{n\beta} = \mathrm{H}_n^{(2)}(k_\beta r)$ and $B_n = k_\beta^n H_{n\beta} - k_\alpha^n H_{n\alpha}$.

3.2 Domain decomposition for modeling thin structures

The approach used here to model wave propagation around a thin structure (crack or rigid screen) is based on the decomposition of the domain in two different sub-domains, as illustrated in Figure 2. If the thin structure is a rigid screen located in an acoustic domain, the interface between the two sub-domains will be a curve, designated as C, containing the thin structure, T, and a fictitious interface, named F. In order to correctly describe the behavior of the thin screen, null particle velocities must be ascribed to both sides of the screen (T) and continuity of pressure and velocity should be imposed along F.

A similar procedure should be followed when the thin structure is a crack located inside an elastic medium, for which case boundary conditions of null stresses (for a crack) should be ascribed to both sides of the interface T, while continuity of both displacements and stresses must be enforced along F. This situation is schematically represented in Figure 3.

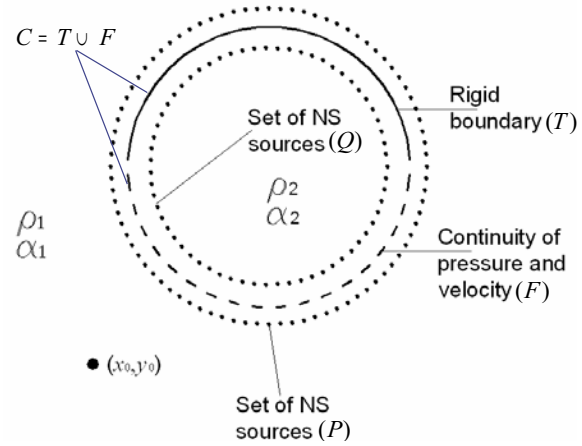

Figure 2: Schematic representation of the domain decomposition for an acoustic medium.

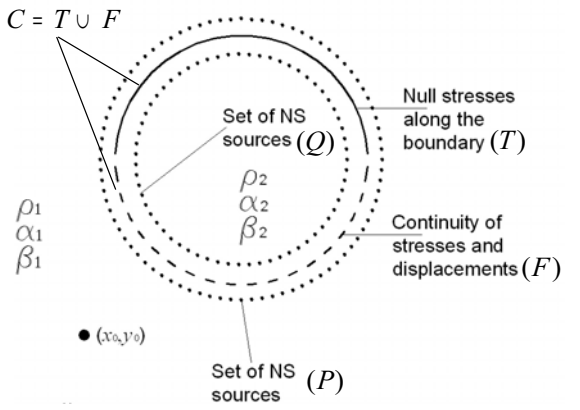

Figure 3: Schematic representation of the domain decomposition for an elastic medium.

4 Performance of the proposed MFS approach

The above-defined formulations have been implemented in computer codes, and their accuracy tested by comparing the results they provide with alternative numerical formulations. For the purpose of this comparison, a Traction Boundary Element code was used as a reference, since it a very accurate approach that allows very efficient analysis of wave propagation around cracks and rigid thin structures, requiring only the discretization of these discontinuities. For the sake of brevity, the formulation of this method will not be described here. However, it is described in detail in Amado Mendes et al (2006) and Tadeu et al (2006).

In the next sub-sections, a detailed comparison between the results given by the MFS domain decomposition technique and the reference solutions will be given, so that the accuracy and applicability of the proposed approach can be assessed.

4.1 Acoustic wave propagation

Figure 4 gives a schematic representation of the test problem. For this problem, a semi-circular rigid thin screen with a radius of 1.0m is assumed to be located inside an infinite acoustic medium (which is taken to be water). The screen is illuminated by a 2D source (=0.0 rad/m), placed at x=-2.0m and y=0.1m, while the response is calculated at a receiver located at x=0.5m and y=0.5m.

The response computed at this receiver, for 100 frequencies ranging from 20 Hz and 2000 Hz, using the TBEM formulation with 300 elements (used as a reference), is represented in Figure 5.

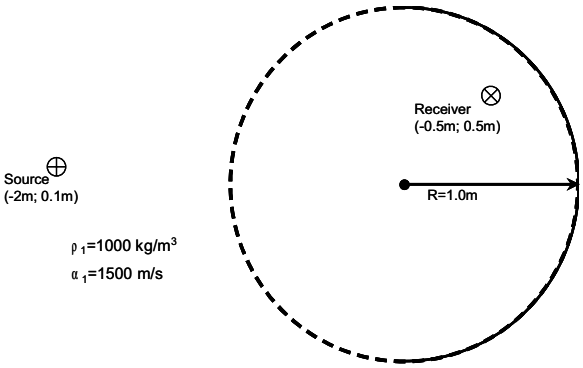

Figure 4: Geometric configuration analyzed.

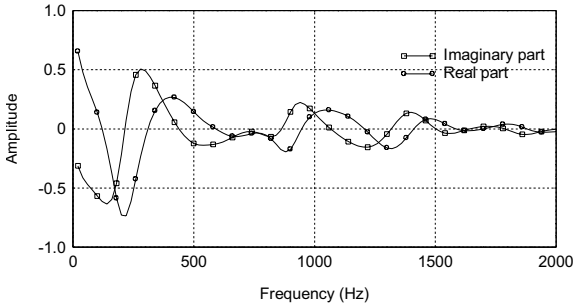

Figure 5: Solution computed using 300 traction boundary elements.

Figures 6, 7, 8 and 9 present the error occurring when the response is computed using the MFS domain decomposition technique, with the fictitious sources placed at 0.05xR, 0.15xR, 0.25xR and 0.35xR from the boundary. In these figures, the error is represented as a 3D plot, with a logarithmic scale on the vertical axis, and one horizontal axis representing the excitation frequency and the other representing the number of collocation points used. For smaller distances, the response seems to become more accurate as the number of collocations points increases, for the full frequency domain. Figures 6 and 7 show that when

the distance from the sources to the boundary is very small the technique is less accurate. Comparing these two figures, the difference between the error amplitudes is very significant, with much better results being obtained when the distance is set to 0.15xR. As the distance to the boundary increases further, an alteration in the results becomes apparent: error peaks occur at high frequencies and there is a greater number of collocation points (see Figure 8). This behavior is much more pronounced for a distance of 0.35xR, when the response obtained with more than 150 collocation points is nearly unusable (Figure 9). In fact the equation system generated for these settings is less well conditioned, and so the results are inaccurate.

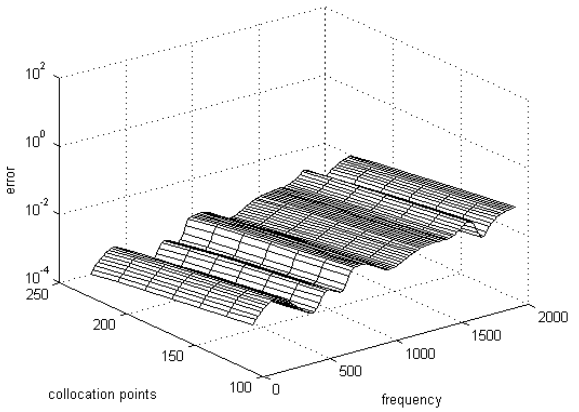

Figure 7: Error from using the MFS with sources placed 0.15xR from the boundary.

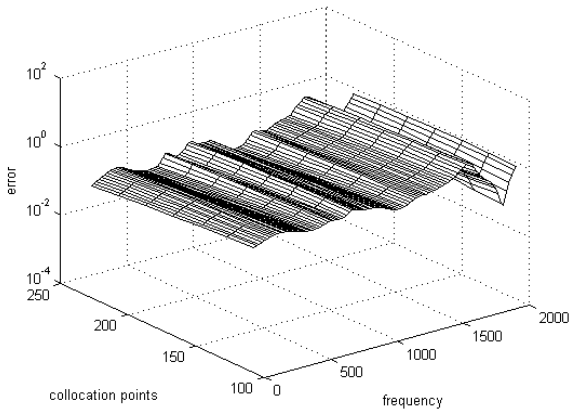

Figure 6: Error for the MFS with sources placed 0.05xR from the boundary.

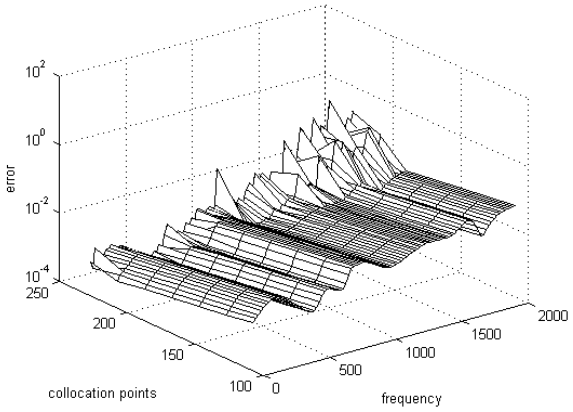

Figure 8: Error from using the MFS with sources placed 0.25xR from the boundary.

To have an objective quantification of the global accuracy of the results, the RMS of the error has been computed along the analyzed frequency domain for each combination of collocation points and distance to the boundary. For this purpose, the RMS error is defined as

$$\varepsilon_{RMS} = \sqrt{\frac{\sum_{i=1}^{NF} (p_i - \overline{p}_i)^2}{NF}}, \qquad (15)$$

where NF is the number of computed frequencies, p_i is the pressure calculated for the MFS for the i^{th} frequency, and $\overline{p}_i$ is the reference solution for the same frequency, computed using the TBEM.

The corresponding results are displayed in Figure 10. This plot clearly shows that there is a region of optimal performance for intermediate distances between sources and boundary, between 0.1xR and 0.2xR. For this distance range, the results provided by this technique are accurate, and seem to converge to the response computed using the TBEM as the number of collocation points increases. Outside this region, the RMS error quickly increases, especially for larger distances and higher numbers of collocation points.

The same analysis was also performed for the case when the source has a sinusoidal variation along the Z axis, defined by k_z=0.5 rad/m. For

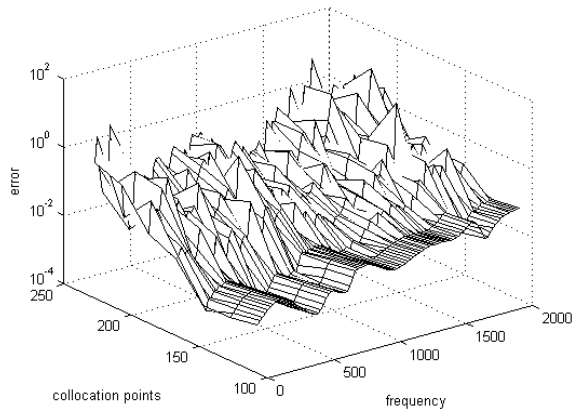

Figure 9: Error from using the MFS with sources placed 0.35xR from the boundary.

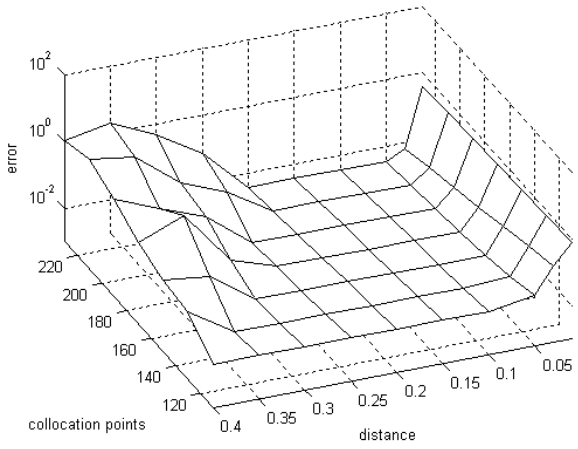

Figure 10: RMS of the error in the frequency domain, for different numbers of collocation points and for different distances from the sources to the boundary.

this source type, the reference solution computed using the TBEM formulation with 300 elements is displayed in Figure 11a, while the RMS error computed in the frequency domain for different numbers of collocation points and for different distances between the virtual sources and the boundary is displayed in Figure 11b. The RMS error computed for the different combinations of distances/collocation points shows a similar behavior to that previously observed for k_z=0.0 rad/m. In fact, a valley is once more clearly visible in the 3D plot, corresponding to a region of optimal performance. Again, this occurs for distances between the sources and the boundary of 0.1xR to 0.2xR, for which the accuracy increases smoothly with the number of collocation points.

4.2 Elastic wave propagation

A large number of tests has been run to study the efficiency of the method in the analysis of wave propagation around a thin crack inside an elastic domain. The most relevant results obtained are presented below. Figure 12 shows the geometric configuration and the physical properties used in these tests, with a semi-circular crack of radius 0.2m located inside an otherwise infinite and homogeneous elastic medium. The propagation domain has been decomposed into two subdomains, with equivalent physical properties. A 2.5D source oscillating at frequencies between 40 Hz and 4000 Hz is placed in the outer domain, illuminating this system. The response is computed at a single receiver, also placed in the outer medium, at x=-0.2 m and y=0.2 m.

Figures 13a and 13b show the reference response (in terms of X and Y displacements, respectively) computed for a source characterized by k_z=0.0 rad/m (2D case) using a TBEM formulation with 300 elements.

Figures 14a and 14b depict the RMS of the error computed in the frequency domain. As in the previous sub-section, these 3D plots use a logarithmic scale on error axis (z), while linear scales are used on the x (number of collocation points) and y (distance from the sources to the boundary) axes. Both plots exhibit very similar shapes, with larger errors obtained for sources placed very close to the boundary and for sources placed further away from it. A valley shaped region, with lower error levels, can be clearly identified, indicating that the most accurate results may be obtained when the fictitious sources are placed at intermediate distances. Within this region, the results seem to improve as more collocation points are used. As in the previous section, the best results seem to be obtained for distances between 0.1xR and 0.2xR.

It is also interesting to see that the error level increases significantly for larger distances between

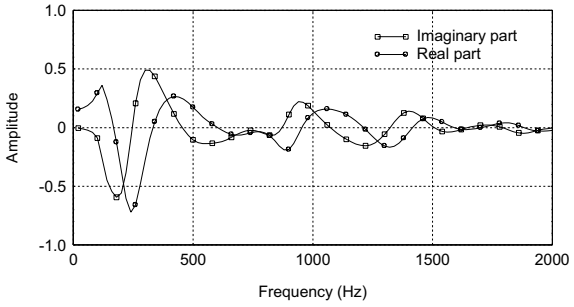

(a)

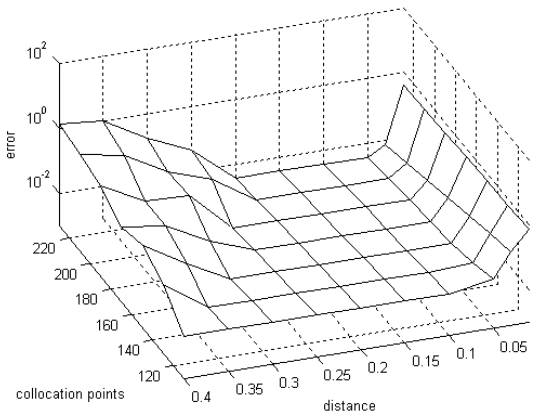

(b)

Figure 11: Results for k_z =0.5 rad/m: a) Reference solution; b) RMS of the error along the frequency domain.

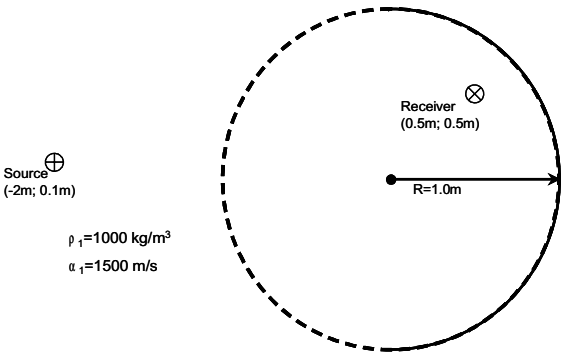

Figure 12: Geometry of the problem.

sources and boundary when the number of collocation points also increases. In this case, the increasing number of collocation points starts originating an ill-conditioned, thus reducing the accuracy of the results.

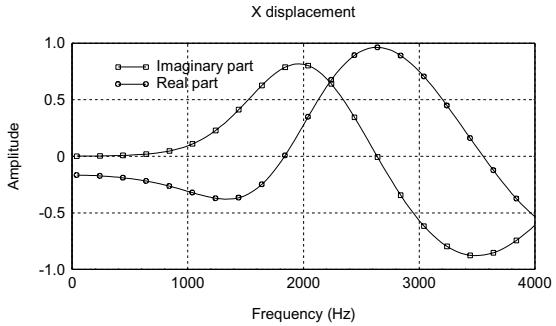

(a)

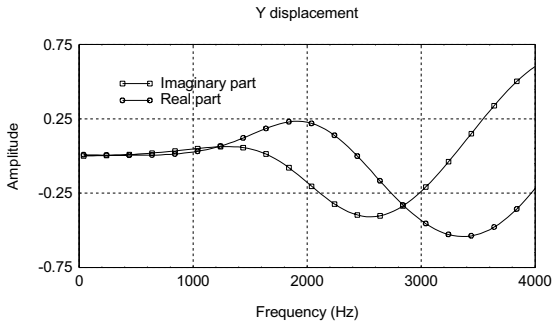

(b)

Figure 13: Results computed using 300 traction boundary elements: a) X displacement; b) Y displacement.

In the examples presented here, only the case where the axial wavenumber k_z=0.0 rad/m, corresponding to a 2D problem. However, other results obtained in complementary testing (not shown) indicate a similar behavior of the method for distinct values of k_z.

5 Numerical application example

To show the applicability of the methodology to analyze wave propagation around a thin structure, a numerical example is presented below. It consists of a rigid screen placed in an infinite fluid medium. The fluid is assumed to be water, with a density of 1000 kg/m^3, allowing an acoustic wave propagation velocity of 1500 m/s. The thin screen has a circular shape, as defined in Figure 15, with a small opening 0.5 m wide. This system is excited by a line source placed at x=-0.9 m

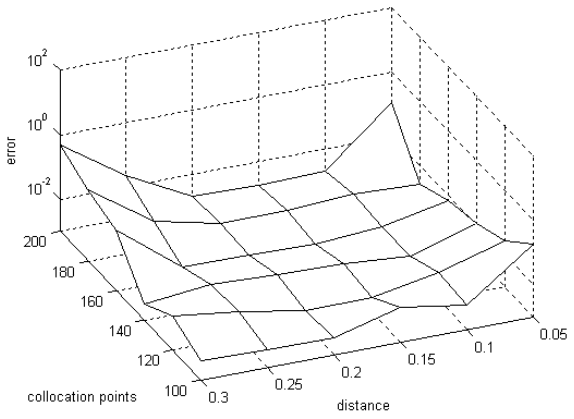

(a)

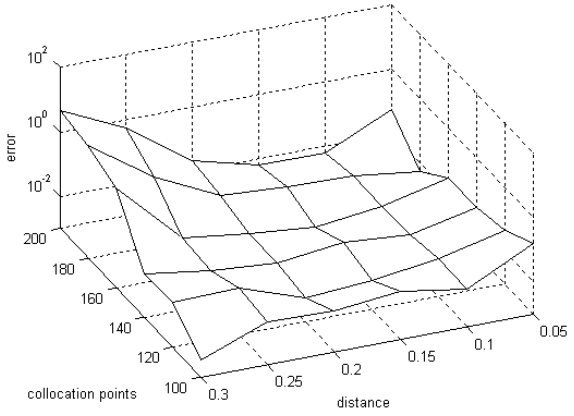

(b)

Figure 14: RMS of the error committed when using the MFS along the frequency domain: a) X displacement; b) Y displacement.

and y=0.0 m. Responses have been computed over a square grid of 50x50 receivers, equally spaced between x=-2.0 m ; y=-2.0 m and x=2.0 m ; y=2.0 m, for a full range of frequencies from 20 Hz and 2560 Hz. These responses have been transformed to the time domain, assuming that the line source emits a Ricker pulse [Tadeu et al (1999)] with a central frequency of 1000 Hz. In this process, complex frequencies of the form $\omega_c = \omega - i\eta$, with $\eta = 0.7\Delta\omega$, are used to prevent the "aliasing" phenomenon.

A number of snapshots, which illustrate the wave propagation within this region, are displayed in Figure 16.

At time t=0 ms, the source emits a Ricker pulse

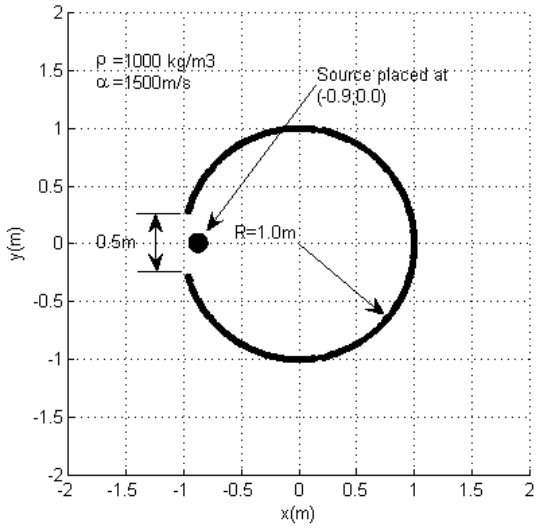

Figure 15: Schematic representation of the problem's geometry.

which propagates away from it. Part of the corresponding wavefront then hits the inner boundary of the screen, where it is reflected back to the interior part of the domain. At the same time, another part of the wavefront passes through the small opening, and is diffracted at its edges to generate a larger wavefront. This behavior can clearly be seen in Figure 16a, where a snapshot taken at t=2 ms is displayed. The generated wavefronts continue to propagate through the domain, with more reflections being generated within the confined domain. The outer wavefront propagates around the rigid screen, even reaching receivers placed in the shadowed zone behind the screen (see Figure 16b, for t=6 ms). At later times, the multiple reflections that occur within the confined space also reach the opening, generating new wavefronts that propagate in the domain surrounding the rigid screen, such as the ones that are visible in the Figure 16c snapshot, taken at t=14 ms.

Examination of the above pictures shows that the presented simulation is consistent with the behavior expected of the system, indicating a very good behavior of the approach used here for the study of wave propagation around a rigid screen.

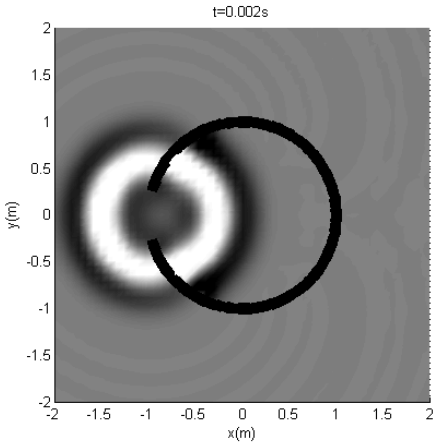

(a)

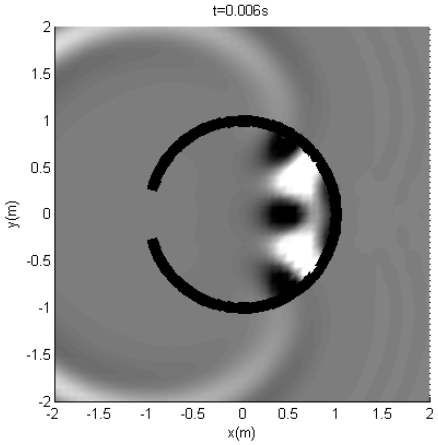

(b)

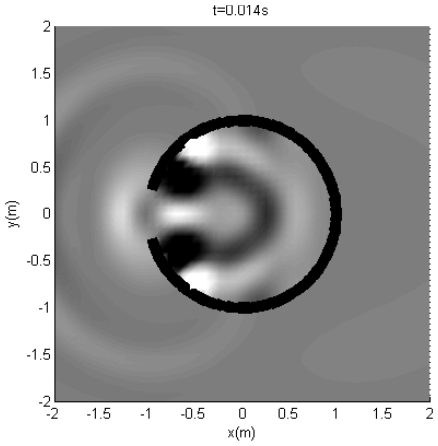

(c)

Figure 16: Snapshots taken for different time instants.

6 Conclusions

A numerical strategy, based on domain decomposition, has been used to simulate the propagation of waves in an acoustic and an elastic medium containing thin structures, such as rigid screens or empty cracks, using the Method of Fundamental Solutions. The results provided by this method were compared with reference solutions computed using a Traction Boundary Element formulation, making it possible to conclude that the technique provides very good results if the virtual sources are judiciously placed at specific distances from the boundaries. For a circular geometry, the authors conclude that the best results are obtained when these virtual sources are at a distance of approximately 0.1xR to 0.2xR from the boundary. This conclusion was valid both for elastic and for acoustic domains. It was also possible to conclude that, for larger distances, when a very large number of collocation points is used, the response diverges, possibly because an ill-conditioned equation system is generated. The authors also conclude that when the sources are too close to the boundary the results are less accurate.

A numerical example of application was also presented, clearly showing that the methodology is applicable to the case of a circular rigid screen located inside a fluid medium.

References

Alves, C.J.S. and Leitão V.M.A.(2006): Crack analysis using an enriched MFS domain decomposition technique*, Eng. Analysis Bound. Elements* 30 (3), 160-166.

Amado Mendes, P. & Tadeu, A. (2006). Wave propagation in the presence of empty cracks in an elastic medium. Computational Mechanics, vol. 38(3), pp. 183-199.

Atluri, S.N. (2004): *The Meshless Method (MLPG) for Domain & BIE Discretizations*, Tech Science Press.

Fairweather, G., Karageorghis, A. (1998): The method of fundamental solutions for elliptic boundary value problems, *Advances in Comp.*

Math., Vol. 9, pp. 69 95.

Godinho, L., Tadeu, A., Branco, F. (2003): Wave scattering by infinite cylindrical shell structures submerged in a fluid medium, *Wave Motion Journal*, Vol. 38, No.2, pp. 131-149.

Godinho, L.M.C., Tadeu, A., Simões, N.A. (2006): Accuracy of the MFS and BEM on the analysis of acoustic wave propagation and heat conduction problems, To appear in J. Sladek, V. Sladek, and S.N. Atluri (Eds.), *Advances in the Meshless Method: 2005*.

Golberg, M.A., Chen, C.S. (1999): The method of fundamental solutions for potential, Helmholtz and diffusion problems, In: *Boundary Integral Methods: Numerical and Mathematical Aspects*, M.A. Golberg, editor, WIT Press & Computational Mechanics Publications, Boston, Southampton, pp. 103-176.

Kansa, E.J. (1990): A Scattered data Approximation Scheme with Applications to Computational Fluid Dynamics II, *Comput Math Appl*, Vol. 19, No. 8/9, pp. 147-61.

Tadeu, A., Amado Mendes, P., António, J. (2006). 3D elastic wave propagation modelling in the presence of 2D fluid filled thin inclusions. *Engineering Analysis with Boundary Elements*, vol. 30(3), pp. 176-193.

Tadeu, A., Kausel, E. (2000): Green's functions for two-and-a-half dimensional elastodynamic problems, *Journal of Engineering Mechanics, ASCE*, Vol 126(10), pp. 1093-1097.

Tadeu, A., Godinho, L. (1999): 3D Wave Scattering by a Fixed Cylindrical Inclusion in a Fluid Medium, *Engineering Analysis with Boundary Elements*, Vol. 23, pp. 745-756.

Tadeu, A., Santos, P., Kausel, E. (1999): Closed-form Integration of Singular Terms for Constant, Linear and Quadratic Boundary Elements -Part I: SH Wave Propagation, *Eng. An. Bound. Elmts*., Vol. 23 (8), pp. 671-681.

Tadeu, A., Santos, P., Kausel, E. (1999): Closed-form Integration of Singular Terms for Constant, Linear and Quadratic Boundary Elements -Part II: SV-P Wave Propagation, *Eng. An. Bound. Elmts*, Vol. 23 (9), pp. 757-768.